scientific reports

Check for updates

OPEN

Differential microRNA expression profiles and predicted miRNA–mRNA regulatory networks in human macrophage-like cells infected with *Leishmania infantum*

Aurora Diotallevi[1], Gloria Buffi[1], Sara Maestrini[1], Germano Castelli[2], Federica Bruno[2], Fabrizio Vitale[2] & Luca Galluzzi[1]✉

MicroRNAs (miRNAs) regulate gene expression and play a crucial role in numerous diseases, including infections. Leishmaniasis is a neglected infectious disease occurring in different forms (i.e., cutaneous, mucocutaneous, and visceral) caused by a protozoan belonging to the *Leishmania* genus. The parasite infects mainly the macrophages, establishing a niche permissive for its proliferation. *Leishmania* parasites are known to modulate host gene expression, including miRNAs; however, the specific role of these miRNAs in driving host transcriptomic changes remains to be fully characterized. The aim of this work was to study miRNA expression profile in human macrophage-like cells infected by *L. infantum*, the causative agent of visceral and cutaneous leishmaniasis in the Mediterranean region. Moreover, we attempted to identify putative miRNA-mRNA interactions based on the mRNA expression changes previously described. To this end, small RNA-seq was performed in U937 cells infected with *L. infantum* after 24 h and 48 h, and differentially expressed miRNA were identified and validated through qPCR. For identifying miRNA-mRNA interactions, the upregulated and downregulated miRNAs at 24 h ($n = 24$, 10) and 48 h ($n = 25$, 12) post-infection were analyzed against downregulated and upregulated mRNA, respectively, through the mirDIP (microRNA Data Integration Portal) database. A large fraction of dysregulated protein-coding transcripts was predicted to be affected by dysregulated miRNAs identified in the same samples. We focused in particular on protein-coding genes involved in previously identified dysregulated pathways characterizing *L. infantum* infection (i.e., cholesterol and lipid metabolism, VEGF-VEGFR2 and NF2EL2-related pathways) and transcription factors (TFs). Notably, the fraction of protein coding transcripts predicted to be targeted by dysregulated miRNAs was particularly high in TFs, indicating that changes in a small set of miRNAs may have great impact on macrophage expression profile and phenotype.

Keywords *Leishmania infantum*, Host-parasite interaction, miRNA, Differential expression, Network analysis

Leishmaniasis is a neglected tropical disease caused by protozoan parasites of the genus *Leishmania*. The clinical manifestations range from self-limiting cutaneous lesions to life-threatening visceral forms. The parasites infect mainly host macrophages, subverting host's defense mechanisms and promoting their own replication into the parasitophorous vacuole. This can be accomplished through the modulation of host gene expression, in part by host micro-RNAs (miRNAs)[1]. MiRNAs are short non-coding RNAs that exert post-transcriptional control over gene expression, shaping cellular programs such as differentiation, apoptosis, and immune response. Current evidence suggests that the miRNA-induced silencing effects is largely due to target mRNA degradation, although silencing can also occur through different mechanisms such as inhibition of translation without affecting mRNA stability[2,3].

[1]Department of Biomolecular Sciences, University of Urbino Carlo Bo, Urbino, Italy. [2]OIE Leishmania Reference Laboratory, Centro di Referenza Nazionale per le Leishmaniosi (C.Re.Na.L.), Istituto Zooprofilattico Sperimentale della Sicilia, Palermo, Italy. ✉email: luca.galluzzi@uniurb.it

In the context of *Leishmania* infection, miRNAs represent critical nodes in the molecular dialogue between host and pathogen, influencing immune signaling and potentially being hijacked to favor parasite survival[4]. Several studies were conducted in the last years with different *Leishmania* species and infection models, showing that modulation of miRNAs participates in transcriptomic changes induced by *L. major*[4,5], *L. donovani*[6], *L. infantum*[7–9], *L. braziliensis*[10], and *L. amazonensis*[11,12]. Notably, a broader "cytokine–miRNA" regulatory framework has been described, where *Leishmania* modulates miRNA that influence cytokine/chemokine production, and cytokines (e.g., TGF-β) can regulate the expression of miRNAs in macrophages, influencing the balance of pro- and anti-inflammatory response[13]. Recently, Gharsallah et al. [14] identified potential miRNA target genes involved in key biological processes in *L. amazonensis*-infected murine bone marrow-derived macrophages. In particular, the authors predicted the existence of a large miRNA-mRNA network affecting the expression level of numerous transcription factors, proposing regulatory loops between miRNAs and transcription factors and suggesting miRNAs as candidate regulators whose roles still require functional validation.

Despite these advances, research focusing on host miRNA dynamics in *L. infantum*-infected human macrophages remains limited. In fact, previous studies focused on a few specific miRNAs and/or murine cells/animal models[7,8] and did not focus on comprehensive miRNA-mRNA interactions. A recent paper reported the modulation of mRNA, miRNA and long non-coding RNA expression in human neutrophils in vitro, identifying many differentially regulated transcripts whose interactions appeared to impair phagocytosis, apoptosis and nitric oxide production[9]. However, the information focusing on the interaction between miRNAs and mRNA encoding transcription factors or proteins involved in metabolic pathways is still limited. In this study, we provide a comprehensive small RNA-seq analysis of U937-derived human macrophage-like cells infected with *L. infantum* at 24 h and 48 h, with the aim to identify miRNAs differentially expressed upon infection. Moreover, by integrating miRNA expression profiles with previously obtained mRNA transcriptomics data from the same total RNA samples, we aimed to infer miRNA–mRNA regulatory networks, with particular focus on miRNA-mediated regulation of transcription factors—key orchestrators of macrophage gene expression and phenotype. It is worth noting that this study uses the in vitro differentiated monocytic cell line U937 at early time points post-infection, thus representing a simplified model compared to the multifaceted nature of in vivo infection.

Results and discussion

Identification of dysregulated miRNAs

The selected upregulated miRNAs at 24 h ($n=24$) and 48 h ($n=25$), and downregulated miRNAs at 24 h ($n=10$) and 48 h ($n=12$) are depicted in Fig. 1A and listed in Tables 1, 2, 3 and 4. These lists were compared using InteractiVenn[15], finding several miRNAs commonly dysregulated at both time points (Fig. 1B). The 10 commonly upregulated miRNA at 24 h and 48 h post-infection were: hsa-miR-320c, hsa-miR-1246, hsa-miR-125b-5p, hsa-miR-29b-3p, hsa-miR-100-5p, hsa-miR-17-3p, hsa-miR-146a-5p, hsa-miR-642a-5p, hsa-miR-29a-3p, hsa-miR-32-5p. The 3 commonly dowregulated miRNA at 24 h and 48 h post-infection were: hsa-miR-615-3p, hsa-miR-1301-3p, hsa-miR-223-3p. The miRNA hsa-miR-19b-3p resulted downregulated at 24 h and upregulated at 48 h post-infection. Therefore, aside consistently dysregulated miRNAs at the two time points, miRNA expression appeared to change over time post-infection as observed in several studies across different *Leishmania* species. In fact, many miRNAs can be rapidly up- or downregulated as part of the immediate host response to parasite entry[4,5].

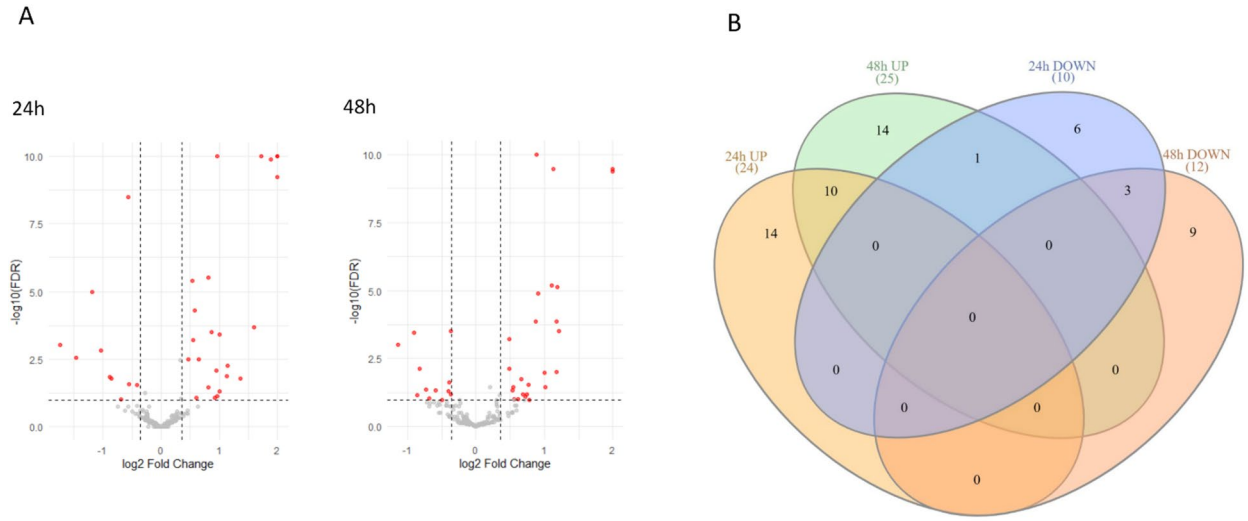

Fig. 1. Volcano plot (**A**) and Venn results (**B**) of dysregulated miRNAs in U937 cells at 24 h and 48 h post-infection. In volcano plot, values exceeding + 2 (log2FC) or −log10(FDR) > 10 were truncated for visualization. The Venn diagram illustrates the number of miRNAs whose expression is significantly altered at 24 h and 48 h following infection with *L. infantum*. Overlapping regions include miRNAs that are commonly dysregulated at different time points, while non-overlapping regions indicate miRNAs uniquely affected in that condition.

miRNA	HGNC symbol	log2 FC
hsa-miR-8485	MIR8485	10.26
hsa-miR-642a-5p	MIR642A	3.41
hsa-miR-1246	MIR1246	2.79
hsa-miR-100-5p	MIR100	1.89
hsa-miR-125b-5p	MIR125B1/MIR125B2	1.73
hsa-let-7d-3p	MIRLET7D	1.60
hsa-miR-1180-3p	MIR1180	1.37
hsa-miR-17-3p	MIR17	1.14
hsa-miR-4286	MIR4286	1.13
hsa-miR-503-3p	MIR503	1.01
hsa-miR-181b-5p	MIR181B1	1.01
hsa-miR-29a-3p	MIR29A	0.96
hsa-miR-486-5p	MIR486	0.96
hsa-miR-193a-5p	MIR193A	0.96
hsa-miR-32-5p	MIR32	0.92
hsa-miR-181a-5p	MIR181A1	0.87
hsa-miR-320c	MIR320C1	0.81
hsa-miR-423-3p	MIR423	0.81
hsa-miR-222-3p	MIR222	0.65
hsa-miR-29b-3p	MIR29B2	0.61
hsa-miR-146a-5p	MIR146A	0.59
hsa-miR-155-5p	MIR155	0.55
hsa-miR-92a-3p	MIR92A1/MIR92A2	0.54
hsa-miR-425-5p	MIR425	0.47

Table 1. Significantly (FDR ≤ 0.1) upregulated miRNA after 24 h infection ($n = 24$).

miRNA-seq validation by RT-qPCR

Five miRNAs were considered for the validation of RNA-seq results: hsa-miR-1246, hsa-miR-17-3p, hsa-miR-193a-5p, hsa-miR-340-5p and hsa-miR-146b-5p. The first two showed a significant and consistent upregulation both at 24 h and 48 h post-infection, the third appeared upregulated at 24 h post-infection, while hsa-miR-340-5p appeared downregulated after 24 h of infection and did not show significant expression changes after 48 h of infection. Finally, hsa-miR-146b-5p did not show any significant expression change both at 24 h and 48 h post-infection. hsa-miR-1246 is particularly interesting because of its known role in infectious diseases and its functions in the inflammatory pathway, angiogenesis and cell proliferation[16,17]. The miRNA hsa-miR-340-5p was considered because among its targets there are mRNAs encoding proteins involved in the response to ER stress[18](e.g., EIF2AK3/PERK, NFE2L2/NRF2, PHLDA1) and mRNA encoding arginase (ARG1), known to be induced in macrophages with M2 phenotype. Notably, this miRNA was downregulated at 24 h post infection, while EIF2AK3, NFE2L2 and PHLDA1 were significantly upregulated. The miRNA hsa-miR-17-3p was taken into consideration because it was stably upregulated (both at 24 h and 48 h post infection) and involved in several biological processes such as the regulation of cell proliferation, inhibition of apoptosis and the modulation of the inflammatory response[19,20]. The miRNA hsa-miR-193a-5p, upregulated at 24 h post-infection in our model, was reported to have a role in immune regulation and inflammatory responses and was found upregulated in M1-polarized macrophages[21]. The relative quantification results obtained using qPCR, once normalized with hsa-miR-16-5p and RNU48, showed a concordant trend with RNA-seq for all selected miRNAs (Table 5).

miRNA-mRNA interaction networks

The miRNA-mRNA interactions were analyzed using mirDIP, as described in methods. The analysis was performed taking into account target predictions in the top 5% and predicted by at least five different algorithms. This confidence threshold was chosen to minimize false positives while retaining enough targets. Under these conditions, a consistent fraction (24%-45%) of dysregulated mRNA showed predicted interactions with dysregulated miRNAs. Results are summarized in Table 6, while detailed lists of miRNA with their associated mRNA are provided in supplementary Table S1 and S2 for 24 h and 48 h, respectively. The analysis at 24 h (supplementary Table S1) showed that all miRNAs may have multiple predicted targets among dysregulated genes, from 6 (for hsa-miR-1307-5p) up to a maximum of 108 (for hsa-miR-21-5p). At 48 h, the number of predicted targets among dysregulated genes appeared lower, ranging from 1 (hsa-miR-32-5p) to 15 (hsa-miR-125b-5p) (supplementary Table S2). Overall, this analysis allowed to propose miRNAs as potential pleiotropic regulators that may be engaged by *Leishmania* to efficiently reprogram the host cell expression profile, as proposed previously in a different model[14].

miRNA	HGNC symbol	log2 FC
hsa-miR-1246	MIR1246	2.05
hsa-miR-642a-5p	MIR642A	2.04
hsa-miR-210-3p	MIR210	1.21
hsa-miR-100-5p	MIR100	1.19
hsa-miR-29b-3p	MIR29B1/MIR29B2	1.18
hsa-miR-203a-3p	MIR203A	1.17
hsa-miR-125b-5p	MIR125B1/MIR125B2	1.13
hsa-miR-7-5p	MIR7-1	1.10
hsa-miR-32-5p	MIR32	1.01
hsa-miR-17-3p	MIR17	1.00
hsa-miR-148a-3p	MIR148A	0.91
hsa-miR-146a-5p	MIR146A	0.89
hsa-miR-142-3p	MIR142	0.87
hsa-miR-542-3p	MIR542	0.78
hsa-miR-101-3p	MIR101-1	0.77
hsa-miR-30b-5p	MIR30B	0.75
hsa-miR-320c	MIR320C1	0.72
hsa-miR-19b-3p	MIR19B	0.69
hsa-miR-142-5p	MIR142	0.66
hsa-miR-221-5p	MIR221	0.62
hsa-miR-29c-3p	MIR29C	0.55
hsa-miR-629-5p	MIR629	0.54
hsa-miR-20a-5p	MIR20A	0.53
hsa-miR-199a-3p	MIR199A1/MIR199A2	0.49
hsa-miR-29a-3p	MIR29A	0.49

Table 2. Significantly (FDR ≤ 0.1) upregulated miRNA after 48 h infection ($n = 25$).

miRNA	HGNC symbol	log2 FC
hsa-miR-21-5p	MIR21	-0.41
hsa-miR-15a-5p	MIR15A	-0.55
hsa-miR-223-3p	MIR223	-0.56
hsa-miR-1301-3p	MIR1301	-0.68
hsa-miR-615-3p	MIR615	-0.85
hsa-miR-19b-3p	MIR19B	-0.88
hsa-miR-340-5p	MIR340	-1.04
hsa-miR-374a-5p	MIR374A	-1.19
hsa-miR-1307-5p	MIR1307	-1.47
hsa-miR-590-3p	MIR590	-1.74

Table 3. Significantly (FDR ≤ 0.1) downregulated miRNA after 24 h infection ($n = 10$).

Dysregulated miRNAs support enrichment of polarization markers in *L. infantum*-infected U937 cells

While U937 cells provide a standardized model for *Leishmania* infection, their neoplastic origin and PMA-induced differentiation may not fully capture the complex polarization plasticity of primary human macrophages. Nevertheless, our previous mRNA-seq analysis showed that, while *L. infantum*-infected U937 cells did not exhibit a clear polarization phenotype, several M1- and MOX- (a specialized macrophage activation state triggered by oxidative stress)[22] associated transcripts were significantly upregulated at 24 h post-infection[23]. We analyzed potential interactions between these transcripts and downregulated miRNAs using mirDIP as described in Methods. The results showed that 7 out of 10 downregulated miRNA at 24 h were directly predicted to target 10 upregulated M1 or MOX-associated transcripts previously identified[23](Fig. 2).

Moreover, the dysregulated miRNAs included many miRNAs directly or indirectly associated with M1 polarization and inflammatory gene regulation[24]. Among them several are considered "immunomiRs" (e.g. miR-155, miR-146a, miR-17–92, miR-223, miR-181 and miR-21)[25,26]. They are widely expressed in cells of the immune system and regulate critical immune functions. In details, miR-146a-5p and miR-155-5p are abundant in most innate and adaptive immune cells, in which they exert strong regulation of immune response. They are

miRNA	HGNC symbol	log2 FC
hsa-miR-223-3p	MIR223	-0.37
hsa-miR-99b-5p	MIR99B	-0.37
hsa-miR-191-5p	MIR191	-0.39
hsa-miR-342-3p	MIR342	-0.40
hsa-miR-1307-3p	MIR1307	-0.50
hsa-miR-941	MIR941-1	-0.59
hsa-miR-365b-3p	MIR365B	-0.68
hsa-miR-3615	MIR3615	-0.73
hsa-miR-615-3p	MIR615	-0.83
hsa-miR-1976	MIR1976	-0.86
hsa-miR-744-5p	MIR744	-0.91
hsa-miR-1301-3p	MIR1301	-1.14

Table 4. Significantly (FDR ≤ 0.1) downregulated miRNA after 48 h infection ($n = 12$).

miRNA	HGNC symbol	Time post-infection	miRNA-seq Fold Change	miRNA-seq *p*-value	RT-qPCR Fold Change	RT-qPCR *p*-value
hsa-miR-17-3p	MIR17	48 h	2.0	< 0.01	2.75	< 0.01
hsa-miR-1246	MIR1246	24 h	6.9	< 0.001	3.89	< 0.01
hsa-miR-340-5p	MIR340	48 h	1.13	n.s.	1.02	n.s.
hsa-miR-340-5p	MIR340	24 h	0.49	< 0.001	0.68	< 0.05
hsa-miR-193a-5p	MIR193A	24 h	1.94	< 0.001	1.31	< 0.05
hsa-miR-146b-5p	MIR146B	24 h	1.14	n.s.	1.08	n.s.

Table 5. Fold change comparison between miRNA-seq and RT-qPCR analysis in U937 infected cells. n.s.: not significant.

	Upregulated genes	Upregulated genes with predicted interactions with downregulated miRNA (%)	Downregulated genes	Downregulated genes with predicted interactions with upregulated miRNA (%)
24 h	749	339 (45.3%)	864	289 (33.4%)
48 h	124	48 (38.7%)	330	79 (23.9%)

Table 6. Summary of dysregulated mRNA showing predicted interactions with dysregulated miRNAs.

functionally connected, forming a balanced contrast, with miR-146a-5p representing the anti-inflammatory and miR-155-5p the pro-inflammatory part. The miR-17-92 cluster has a role in immune modulation, regulating cytokine signaling pathways, (e.g., TGF-β, IL-6/STAT3 pathways) and influencing macrophage polarization, T cell activation, and immune evasion. In summary, the miR-17-92 cluster acts as a regulator of inflammation in macrophages and plays a role in both promoting and resolving inflammation. The mature miRNAs within this cluster include hsa-miR-17-5p and 3p, hsa-miR-18a-5p, hsa-miR-19a-3p, hsa-miR-19b-3p, hsa-miR-20a-5p, and hsa-miR-92a-3p. Most of them appeared to be upregulated at 24 h and/or 48 h post-infection. Concerning miR-223-3p, it has been shown to be downregulated following stimulation of macrophages, which enhances pro-inflammatory cytokine expression[25]. At 24 h post-infection, this miRNA appeared downregulated while the pro-inflammatory cytokines IL1β and IL6 were upregulated. The miR-181a-5p and miR-181b-5p (upregulated at 24 h in our infection model) are potent anti-inflammatory miRNAs in both mature innate and adaptive immune cells. Finally, miR-21 (downregulated at 24 h in our infection model) has a key role in the resolution of inflammation and in the negative regulation of the pro-inflammatory response, particularly in macrophages, suggesting that miR-21 inhibition in leukocytes promotes inflammation[27]. In summary, concerning the regulation of polarization in macrophage-like cells infected by *L. infantum*, miRNAs expression appears to support a balanced pro-inflammatory and anti-inflammatory response, confirming results previously observed by mRNA-seq on the same samples[23].

Interaction between miRNA and TFs during infection

Among the mRNA dysregulated by infection, many transcription factors were identified. In details, at 24 h, 71 (9.5%) and 39 (4.5%) TFs were identified among the 749 upregulated and 864 downregulated mRNA, respectively. At 48 h, 11 (8.9%) and 6 (1.8%) TFs were identified among the 124 upregulated and 330 downregulated mRNA, respectively. The complete list of dysregulated TFs is shown in supplementary Table S3.

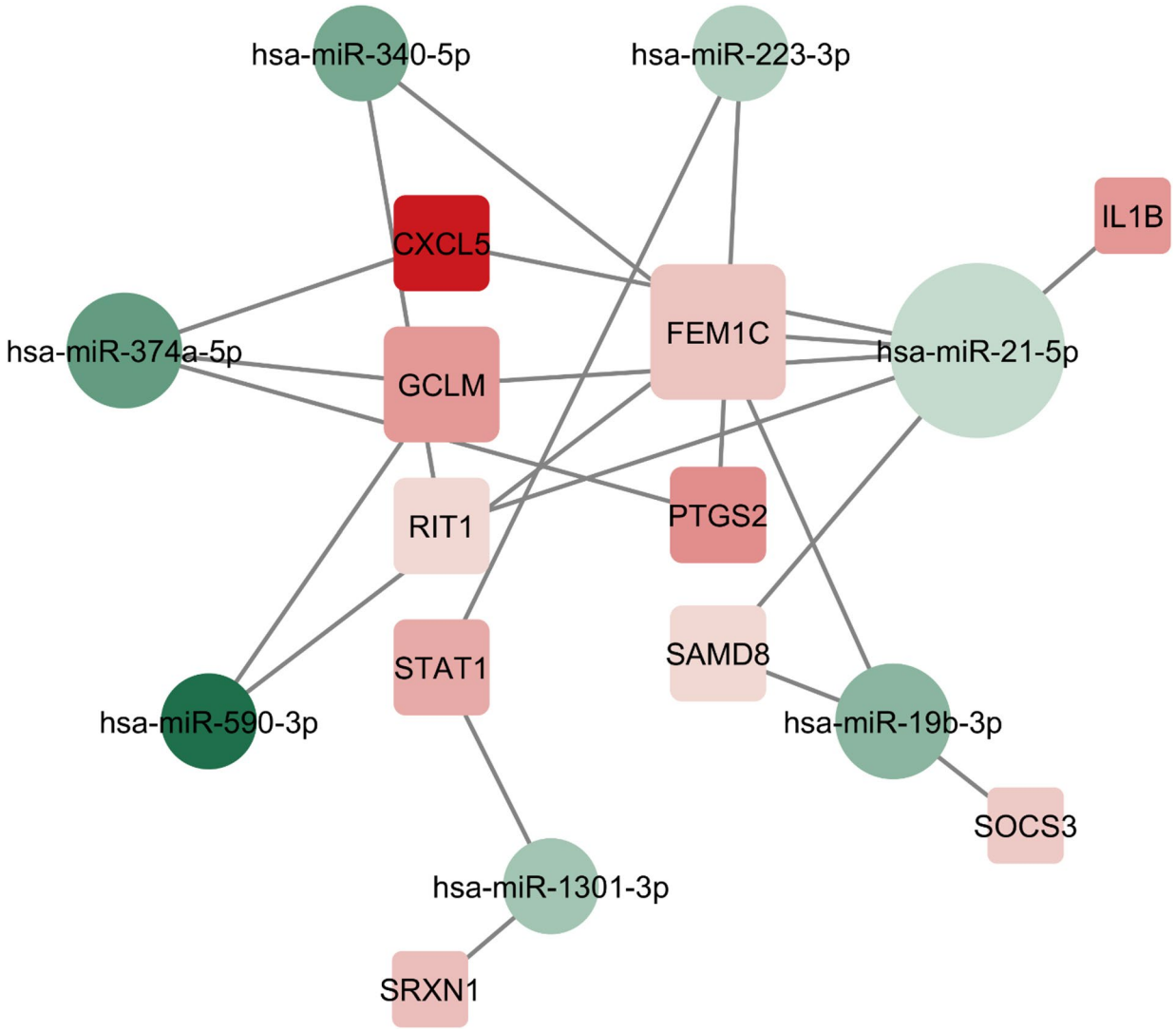

Fig. 2. Predicted direct interactions between upregulated M1 and MOX marker mRNAs and downregulated miRNAs. The miRNAs are depicted as circular nodes and mRNAs as square nodes. Node fill color reflects the $\log_2$ fold-change, with color gradients corresponding to the magnitude of expression changes. Larger nodes represent elements with a higher number of interactions.

It is well established that miRNAs frequently target TFs due to their higher complexity in 3'-UTR regions. This allows fine-tuning of TF translation and implies that the regulation of specific TFs may be a key feature of miRNA function[28,29]. In the context of *Leishmania* infection, the interactions between miRNA and TFs may represent a very efficient immune subversion strategy since changes in few miRNA may have important consequences on macrophage expression profile. This can happen by direct targeting TFs mRNA or by leveraging regulatory loops (feed-forward and feedback) between miRNAs and TFs[30], contributing to explain transcriptomic changes described in U937 cells infected by *L. infantum*[23]. The predicted interactions between miRNA and TFs were analyzed as described in methods. The results of in silico analysis of these interactions are summarized in Table 7. At 24 h post infection, among the 71 upregulated TF, 41 (i.e., 58%) were predicted target of the 10 downregulated miRNAs, and among 39 downregulated TF, 26 (i.e., 67%) were predicted target of 23 out of 24 upregulated miRNAs. At 48 h post-infection, among the 11 upregulated TF, 8 (i.e., 72.7%) were predicted target of 9 out of 12 downregulated miRNAs, and among 6 downregulated TF, 4 (i.e., 67%) were predicted target of 13 out of 25 upregulated miRNAs. Taken together, these analyses suggest a potential interaction between miRNA and TFs dysregulated by *L. infantum* infection, either at 24 h and 48 h. The miRNA-mRNA interactions are shown in Fig. 3 that visualizes networks between up-regulated miRNAs and down-regulated TF mRNAs at 24 h and 48 h (panel A, B), and vice versa between down-regulated miRNAs and up-regulated TFs at 24 h and 48 h (panel C, D).

Notably, some TFs were predicted to be targets of many (≥ 5) dysregulated miRNA. For instance, RUNX1, LCOR, NFAT5 (among the upregulated TF) and EGR3, TFDP2 (among the downregulated TF). RUNX1 is a key transcription factor in macrophages that drives M1 polarization and inflammatory cytokine production[31].

	Upregulated TF	Upregulated TF with predicted interactions with downregulated miRNA (%)	Downregulated TF	Downregulated TF with predicted interactions with upregulated miRNA (%)
24 h	71	41 (57.7%)	39	26 (66.7%)
48 h	11	8 (72.7%)	6	4 (66.7%)

Table 7. Summary of dysregulated mRNA encoding for transcription factors (TFs) showing predicted interactions with dysregulated miRNAs.

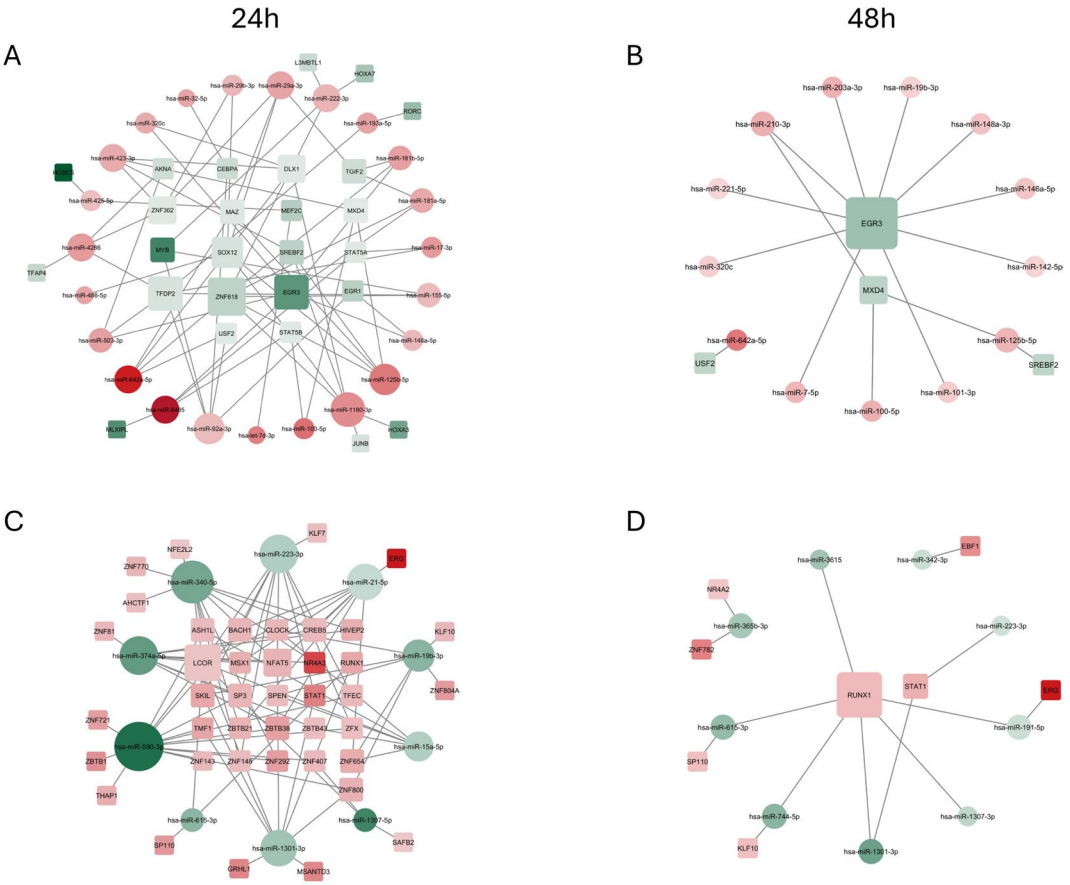

Fig. 3. Predicted interactions between differentially expressed miRNAs and transcription factors (TFs) over time. Interactions between upregulated miRNAs and downregulated TFs are shown in panel A (24 h) and B (48 h), while interactions between downregulated miRNAs and upregulated TFs are shown in panel C (24 h) and D (48 h). The miRNAs are depicted as circular nodes and mRNAs as square nodes. Node fill color reflects the $\log_2$ fold-change, with color gradients corresponding to the magnitude of expression changes. Larger nodes represent elements with a higher number of interactions.

LCOR can act as a transcriptional corepressor and it has been identified as a negative regulator of adipogenesis[32]. It mediates gene silencing by recruiting HDACs and other epigenetic repressors to suppress the expression of genes involved in fatty acid synthesis and storage (e.g., PPARγ/RXRα, which in turn activate SREBF1 and FASN). Recent studies suggest LCOR may also play a role in modulating the immune response, possibly influencing immune evasion mechanisms in cancer by regulating genes involved in antigen processing[33]. By indirectly repressing FASN and SREBF1, LCOR may limit nutrient availability to parasite and suppress lipid mediators (e.g., prostaglandins) that modulate inflammation. NFAT5 regulates the expression of multiple TLR-induced genes in macrophages. It is required for the induction of NOS2, TNF and IL6 mainly under mild stimulatory conditions, indicating that NFAT5 could regulate specific gene patterns depending on pathogen burden intensity. In vivo, NFAT5 was demonstrated to be necessary for effective immunity against *L. major*, whose clearance requires TLRs and iNOS expression in macrophages[34]. EGR3 and TFDP2 are involved in immune regulation and cell cycle progression, respectively. In particular, EGR3 regulates the expression of many genes involved in immune responses and inflammatory processes, such as cytokines (including IL6 and IL8), growth factors, and

matrix remodelling factors[35]. Notably, in immune cells EGR3 typically functions as a negative regulator of the inflammatory response[36].

On the other hand, several miRNA were predicted to regulate many TFs, highlighting their relevance in modulating expression profile. A pleiotropic miRNA among upregulated miRNAs is hsa-miR-1180-3p (predicted to interact with 6 TFs) while among downregulated miRNAs are hsa-miR-223-3p, hsa-miR-340-5p, hsa-miR-374a-5p, hsa-miR-590-3p (predicted to interact with ≥ 10 TFs).

Among upregulated TFs interacting with downregulated miRNAs, RUNX1, STAT1, ERG, SP110 and NR4A2/NR4A3 appeared consistently upregulated at 24 h and 48 h post-infection. STAT1 and RUNX1 are considered drivers of M1 activation in macrophages. In contrast, ERG can act as a gatekeeper of inflammation, helping to prevent excessive activation[37]; NR4A2/NR4A3 have been proposed to counter-regulate the inflammatory response[38] and SP110 has immunomodulatory functions and it switches the death signal from necrosis to apoptosis in the infected macrophages[39]. Therefore, a mixed response including activation and regulatory feedback can be inferred, as mentioned above regarding miRNAs supporting pro- and anti-inflammatory response. A lack of classical macrophage activation and mixed/hybrid response was also shown in earlier studies involving murine or human macrophages infected with *L. infantum* (syn. *L. chagasi*)[40,41].

The downregulated TFs interacting with upregulated miRNAs at both 24 h and 48 h post-infection were EGR3, SREBF2, USF2 and MXD4. The first three are involved in immune regulation, cholesterol synthesis, and fatty acid synthesis, respectively. MXD4 is part of the MYC/MAX/MAD transcriptional network and functions as a MYC antagonist, suppressing the transcription of MYC target genes[42]. Because MYC expression appeared reduced following infection, the concomitant downregulation of its antagonist, MXD4, may represent a compensatory response aimed at mitigating the loss of MYC activity.

The predicted role of miRNA in regulation of cholesterol and lipid metabolism

There is a close relationship among host lipid metabolism and immune response during *Leishmania* infection[43]. The changes in cholesterol levels following internalization of *Leishmania* into the macrophage depend on the balance between cholesterol metabolism, uptake, efflux, and storage, as well as time of infection, the infection model and parasite species. In our model, U937 cells infected by *L. infantum* showed a significant downregulation of cholesterol and lipid metabolism-associated genes, both at 24 h and 48 h post-infection. This is coherent with previous findings in which cholesterol levels in macrophages were shown to decrease following internalization of *Leishmania* parasites. This change has significant implications for host immune function. In fact, low cholesterol is associated with impaired antigen presentation through MHC class II and parasite survival[44].

Regarding cholesterol metabolism, at 24 h 9 out of 22 downregulated genes were predicted to be target of 16 upregulated miRNAs (Fig. 4A). At 48 h, 4 out of 11 downregulated genes were predicted to be target of 5 upregulated miRNAs (Fig. 4B).

Regarding lipid biosynthetic process, at 24 h 20 out of 48 downregulated genes were predicted to be target of 19 upregulated miRNAs (Fig. 4C). At 48 h, 6 out of 22 downregulated genes were predicted to be target of 9 upregulated miRNAs (Fig. 4D). The complete gene lists and predicted miRNA interactions are provided in supplementary Table S4.

Most genes targeted by miRNAs within the cholesterol pathway are also shared with the broader lipid metabolic pathway. In fact, SREBF1 (a master regulator of lipid metabolism) and SREBF2 (an activator of genes involved in cholesterol synthesis and uptake) control several common downstream targets (e.g., HMGCR, the rate-limiting enzyme in cholesterol biosynthesis; HMGCS1, involved in the mevalonate pathway; LDLR, which plays a role in cholesterol uptake). SREBF1 was not found among the targets of upregulated miRNAs, however, it has been shown that LCOR overexpression can silence SREBF1[45]. Moreover, PHLDA1 (significantly upregulated 24 h post-infection), can act as a negative regulator of PPARγ[46] reducing the expression of SREBF1[47]. This, in turn, can contribute to down regulation of FASN and SCD (both involved in fatty acid biosynthesis) among its downstream targets. Therefore, the downregulation of genes involved in cholesterol/lipid metabolism could be a synergistic effect between miRNAs and transcription factors (i.e., LCOR) or signaling proteins (i.e., PHLDA1), which in turn can be modulated by other miRNAs. These data were limited to gene expression monitoring since no direct metabolic measurements were performed.

Several miRNAs appear to act as possible pleiotropic regulators in these pathways (e.g., hsa-miR-125b-5p, hsa-miR-1180-3p, hsa-miR-423-3p, hsa-miR-193a-5p, hsa-miR-29a-3p, hsa-miR-29b-3p). Conversely, some target genes appear to be potentially regulated by several miRNAs. For example, at 24 h SREBF2, a master regulator of cholesterol biosynthesis appears downregulated by three miRNAs (hsa-miR-1180-3p, hsa-miR-125b-5p, hsa-miR-423-3p), HMGCR by five miRNAs (hsa-miR-125b-5p, hsa-miR-155-5p, hsa-miR-29a-3p, hsa-miR-29b-3p, hsa-miR-423-3p) and SCD by six miRNAs (hsa-miR-1246, hsa-miR-125b-5p, hsa-miR-146a-5p, hsa-miR-181a-5p, hsa-miR-181b-5p, hsa-miR-222-3p). At 48 h, MSMO1 and LDLR (involved in cholesterol biosynthetic pathway and cholesterol uptake) appear downregulated by 2 miRNAs (hsa-miR-19b-3p, hsa-miR-20a-5p) and 4 miRNAs (hsa-miR-148a-3p, hsa-miR-19b-3p, hsa-miR-20a-5p, hsa-miR-542-3p), respectively. Notably, ST8SIA4, involved in glycosphingolipid biosynthesis, encodes for a protein that is involved in the synthesis of polysialic acid, which has important roles in both innate and adaptive immune response and its upregulation was associated to M2 macrophage polarization[48]. ST8SIA4 appeared downregulated at both 24 h and 48 h post-infection by 4 miRNAs (hsa-miR-125b-5p, hsa-miR-146a-5p, hsa-miR-181a-5p, hsa-miR-181b-5p) and 7 miRNAs (hsa-miR-125b-5p, hsa-miR-142-5p, hsa-miR-146a-5p. hsa-miR-148a-3p, hsa-miR-199a-3p, hsa-miR-19b-3p, hsa-miR-30b-5p), respectively. Among them, hsa-miR-125b-5p has been also experimentally demostrated[49].

Taken together, the predicted interactions of the upregulated miRNA with downregulated genes involved in metabolism of lipids and cholesterol suggest miRNAs as important regulators during *Leishmania* infection.

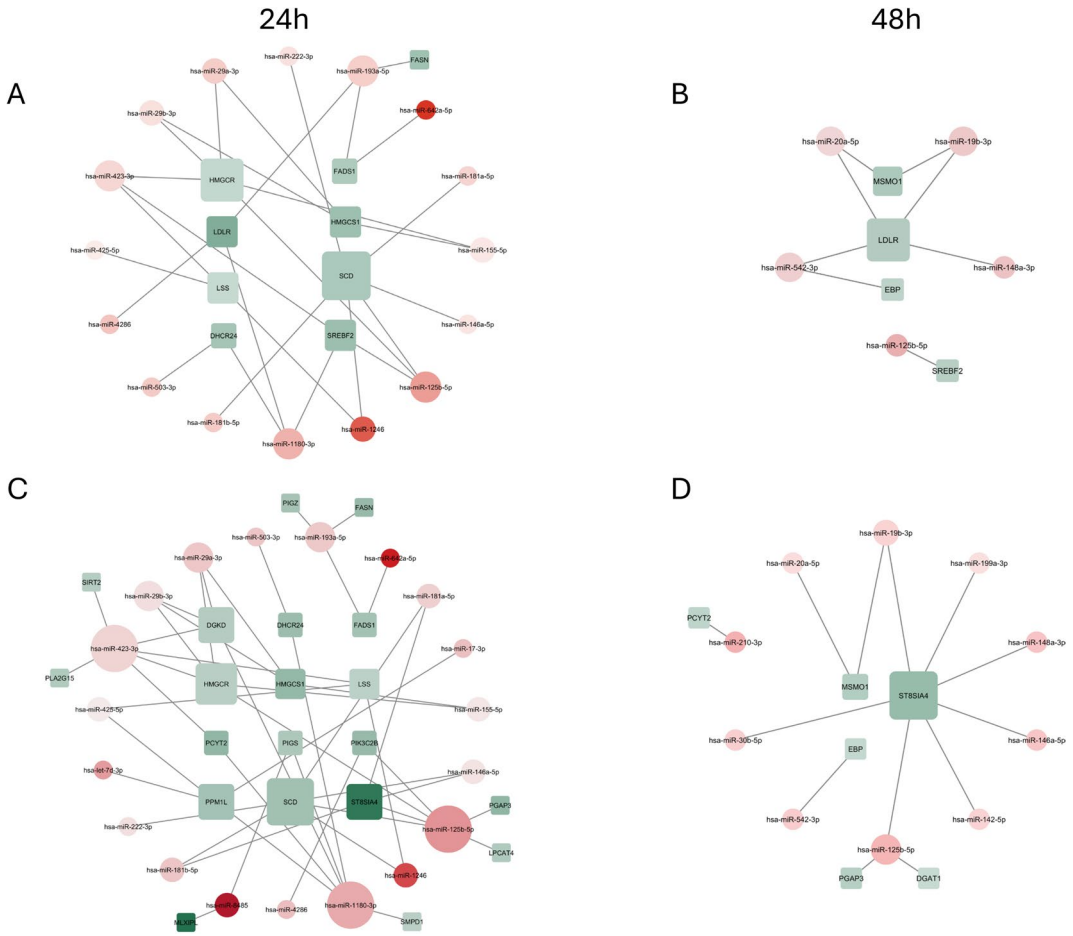

Fig. 4. Predicted interactions between differentially expressed miRNAs and dysregulated target genes. Panel A and panel B refer to networks in cholesterol metabolism, at 24 h and 48 h, respectively, while panel C and panel D refer to the lipid biosynthetic process at 24 h and 48 h, respectively. The miRNAs are depicted as circular nodes and mRNAs as square nodes. Node fill color reflects the $\log_2$ fold-change, with color gradients corresponding to the magnitude of expression changes. Larger nodes represent elements with a higher number of interactions.

The predicted role of miRNA in regulation of the VEGFA-VEGFR2 and NF2EL2-related pathways

We previously observed that the VEGFA-VEGFR2 and NFE2L2-related pathways were significantly enriched among the upregulated genes in *L. infantum*-infected U937 cells at the early time point (24 h)[23]. Therefore, we analyzed interactions among upregulated genes involved in those pathways and downregulated miRNAs at 24 h post-infection. In fact, contrary to cholesterol/lipid metabolism, these pathways were found significantly perturbed at 24 h only.

Concerning NFE2L2 pathways, 15 out of 43 genes were found to be predicted target of 9 out of 10 downregulated miRNAs (only hsa-miR-1307-5p did not match with any upregulated genes) (Fig. 5). Most of the miRNAs involved appeared to regulate more than one target, with the exception of hsa-miR-15a-5p, that was predicted to target HIPK2 mRNA only. On the other side, all upregulated mRNA appeared to be target of ≥2 miRNAs, except for IL1B, NCOA7, PMAIP1, and SRXN1, that were potentially targeted by hsa-miR-21-5p, hsa-miR-374a-5p, hsa-miR-340-5p, and hsa-miR-1301-3p, respectively. In particular, HIPK2, SLC7A11 were predicted to be target of ≥4 downregulated miRNAs. SLC7A11 is a transporter involved in the uptake of cystine, a precursor to glutathione, and in the regulation of ferroptosis[50]. HIPK2 sustains inflammatory cytokine production by promoting endoplasmic reticulum stress in macrophages[51].

Concerning VEGFA-VEGFR2 pathway, 12 out of 20 genes were found to be predicted target of 8 downregulated miRNAs (only hsa-miR-15a-5p and hsa-miR-590-3p target genes did not match with any upregulated genes) (Fig. 6). Among miRNAs with multiple targets, hsa-miR-374a-5p emerged with five predicted targets (FLT1, NR4A3, NUMB, PTGS2, RCAN1). On the other side, several upregulated mRNA appeared to be potential target of a single miRNA. Among the targets regulated by two miRNAs, FLT1, NR4A3, NUMB, PTGS2, and STAT1 emerged. FLT1 (VEGFR1) acts as a receptor for vascular endothelial growth factor (VEGF), also mediating macrophage chemotaxis and inflammation[52]. NUMB, RCAN1 and NR4A3 genes play a role in regulating inflammatory responses in macrophages[38,53], while PTGS2 encodes for an enzyme whose major product is

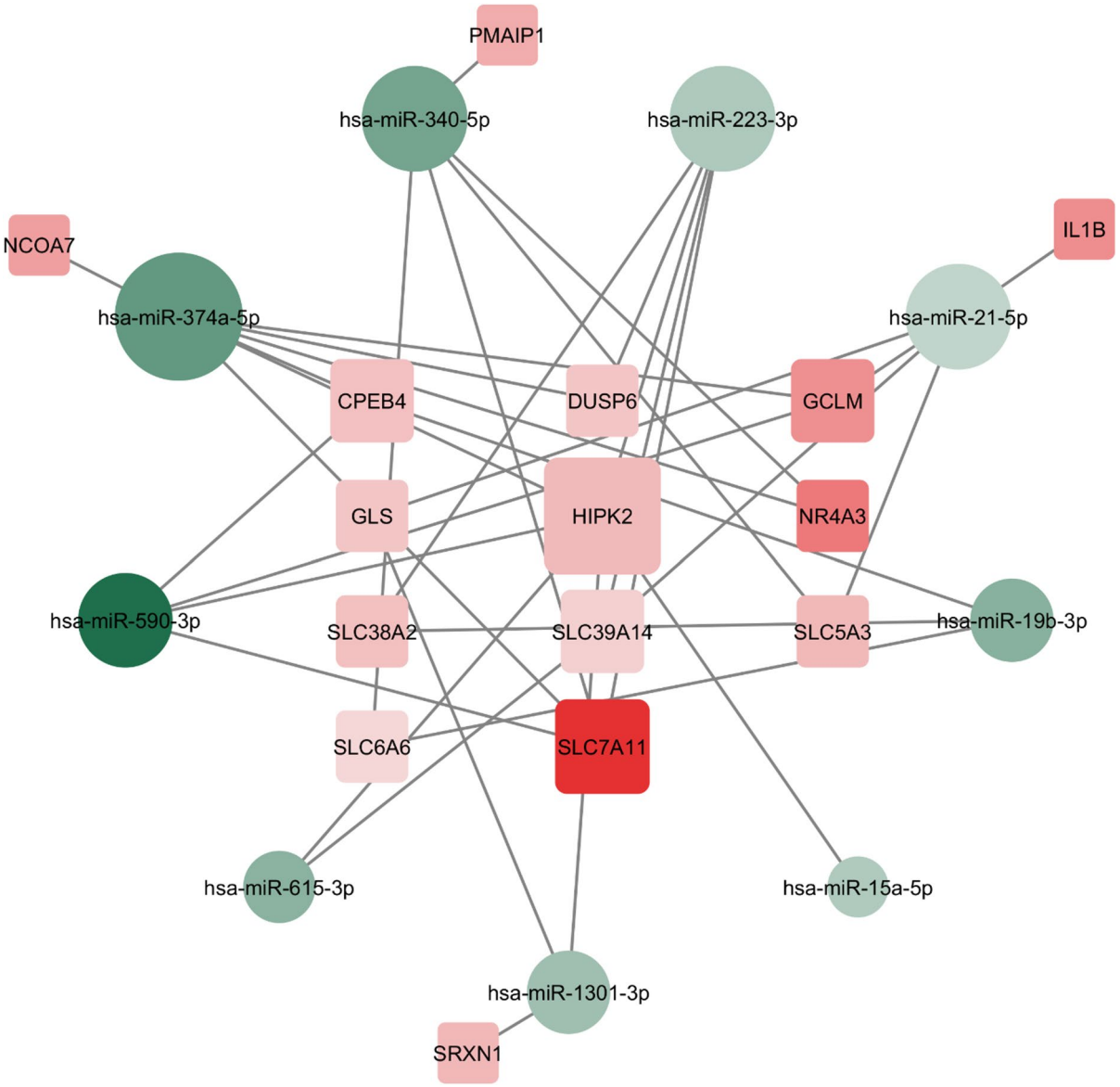

Fig. 5. Predicted interactions between upregulated genes involved in NFE2L2 pathway and downregulated miRNAs. The miRNAs are depicted as circular nodes and mRNAs as square nodes. Node fill color reflects the $\log_2$ fold-change, with color gradients corresponding to the magnitude of expression changes. Larger nodes represent elements with a higher number of interactions.

prostaglandin E2 (PGE2), which promotes inflammation by increasing blood flow and vascular permeability. PTGS2 is upregulated in macrophages during their activation, especially in M1-like macrophages[54]. STAT1 and NR4A3, as well as ERG, are transcription factors that can have different functions other than that of vasculature development (see paragraph Interaction between miRNA and TFs during infection).

Enrichment analysis of predicted miRNA targets among dysregulated mRNAs

To evaluate enrichment of predicted miRNA targets within each gene set, we performed Fisher's exact test using a 2×2 contingency tables. Across the analyzed gene sets, Odds Ratio (OR) values were generally > 1, indicating overrepresentation of predicted miRNA–mRNA interactions, with the exception of the 48 h mRNAdown/miRNAup set (supplementary Figure S1A). Since miRNAs may more frequently target TFs due to their greater 3'-UTR complexity, enrichment analysis for TF-specific gene sets was repeated using a background restricted to TF genes in mirDIP. Although OR values were lower than in the global analysis, they remained > 1. However, due to small number of observations, the 95% CI were wide and statistical significance was not achieved in 2 of the 4 gene sets (supplementary Figure S1B). Overall, the pooled estimates indicate a significant enrichment of miRNA-target interactions.

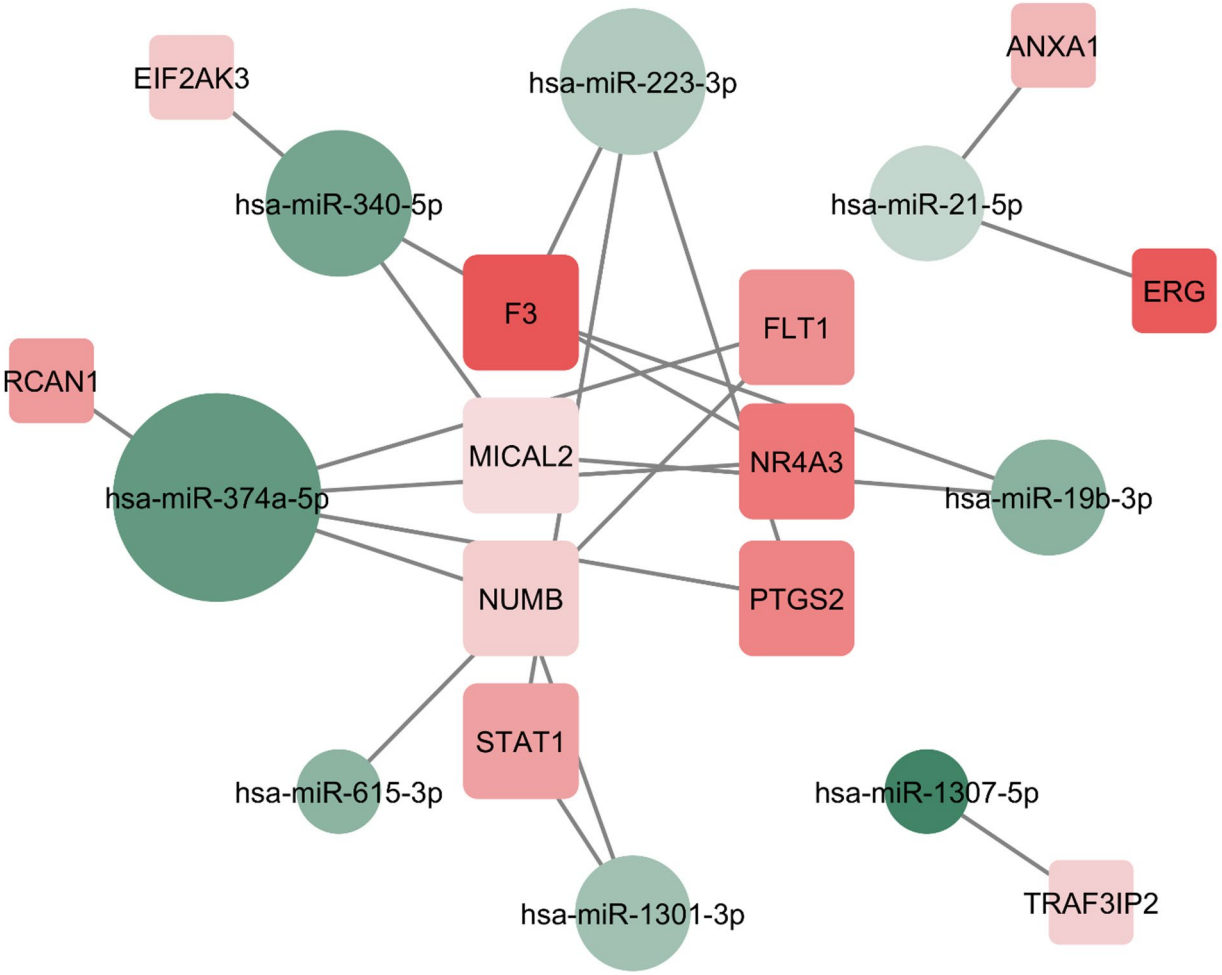

Fig. 6. Predicted interactions between upregulated genes involved in VEGFA-VEGFR2 pathway and downregulated miRNAs. The miRNAs are depicted as circular nodes and mRNAs as square nodes. Node fill color reflects the $\log_2$ fold-change, with color gradients corresponding to the magnitude of expression changes. Larger nodes represent elements with a higher number of interactions.

Conclusions

Applying mRNA-seq and miRNA-seq analysis on U937-derived macrophages infected with *L. infantum*, we gain insight into the potential role of small RNA in modulating host transcriptional immune and metabolic response to infection. In fact, a large fraction of dysregulated protein-coding transcripts was predicted to be affected by dysregulated miRNAs identified in the same samples. Notably, this fraction was particularly high in transcripts encoding transcription factors, indicating that changes in a small set of miRNAs may have great impact on macrophage expression profile and phenotype.

In this view, this work contributes to define miRNAs as possible therapeutic targets against *L. infantum* infection in host cells, with the aim to restore the microbicidal activity of host macrophages, thus avoiding resistance problems arising from parasite-targeted approaches.

It is worth mentioning that the transcriptional regulatory network in macrophages infected by *L. infantum* appears highly complex, and direct mRNA–miRNA interactions provide only a partial perspective, as they fail to capture the broader landscape of indirect regulatory effects. However, identifying key miRNAs involved in immune or metabolic response of infected macrophage could allow to exploit them as therapeutic target using mimic or anti-miR (i.e., synthetic oligonucleotide designed to specifically bind to and inhibit a target miRNA)[55] approaches. Since mRNA-miRNA interactions were predicted in silico based on experimentally observed changes in their expression in a macrophage-like cell line, future studies should focus on experimental validation of these interactions, for example using miRNA mimics and/or inhibitors to study their effect on intracellular parasite survival in primary macrophages or infection models.

Methods

Parasite culture

L. infantum (MHOM/IT/08/31U) promastigotes were cultivated in RPMI-PY medium supplemented with 10% heat-inactivated Fetal Bovine Serum (FBS), 1% glutamine and antibiotic solution (250 µg/ml gentamicin and 500 µg/ml 5-fluorocytosine)[56]. Stationary growth parasites were used for the infections.

U937-derived macrophages, infection and total RNA extraction

In this study, we used the infected cells/samples characterized in our previous work[23], allowing direct comparison and continuity in experimental conditions. Briefly, the human monocytic cell line U937 (ATCC CRL-1593.2) was cultured in RPMI-1640 medium supplemented with 10% Fetal Bovine Serum (FBS), 2 mM L-glutamine, 1% penicillin/streptomycin at 37 °C and 5% CO_2. To induce macrophage differentiation, the U937 cells in the logarithmic phase of growth were plated at the concentration of 6×10^5 cells in 35 mm dishes containing 25 ng/mL of phorbol 12-myristate 13-acetate (PMA) for 18 h. *L. infantum* promastigotes were used to infect U937-derived macrophages with a parasite-to-cell ratio of 5:1. Each infection was repeated twice (i.e., two biological replicates). Non-infected cells treated with PMA were used as control. At 24 h and 48 h post-infection, cells were washed to remove free parasites and directly lysed for downstream analyses. Macrophage-like cells were directly lysed with 700 µl of QIAzol Lysis Reagent (Qiagen, Hilden, Germany). Total RNA extraction was performed with the miRNeasy Mini Kit (Qiagen, Hilden, Germany) following the manufacturer's instructions. To quantify extracted RNA, the Qubit 4 Fluorometer and the RNA HS Assay (Thermo Fisher Scientific, MA, USA) were used. The RNA integrity/quality was preliminarily assessed by 1.2% agarose gel stained with Midori green (Nippon Genetics, Europe).

Small RNA library preparation and sequencing

Library preparation was performed from 100 ng of total RNA using the QIAseq miRNA Library Kit (Catalog no 331502). The libraries were amplified using QIAseq miRNA NGS 12 Index TF (Catalog no 331582). The prepared libraries were quantified using Qubit and assessed for size distribution using the Fragment analyzer (Diatech srl). Libraries were first diluted at 1000 pM concentration, then at 100 pM and pooled together (50 µl each). Finally, 6 µl of pooled libraries were further diluted in a final volume of 100 µl (1:16.7) in dH_2O to obtain 6 pM concentration. The pooled/diluted libraries were loaded on ion 540 chip and sequenced on an ION S5 instrument.

Small RNA-seq analysis

UBAM files were analyzed on the Geneglobe platform at Qiagen using GRCh38 as reference genome and the DeSeq2 normalization method. Reads were processed using UMIs to account for PCR bias. The mapping statistics, including total reads and mapping against the GRCh38 reference genome, are summarized in supplementary Table S5. Differential miRNA expression analysis was performed within the Rstudio statistical environment using the DESeq2 package (1.42.1). UMI counts were imported into a matrix and associated with their respective experimental metadata (condition: infected vs. control, two biological replicates for each condition, either at 24 h and 48 h post-infection). Before statistical analysis, a pre-processing step was implemented to remove low-abundance miRNAs, retaining only features with a total UMI count ≥ 40 across all samples for each time point. Dispersion estimation was conducted using the "local" fitType method, appropriate for the specific nature of this dataset. Statistical testing for the identification of differentially expressed miRNAs was carried out using the Wald test and p-values were adjusted for multiple testing using the Benjamini–Hochberg false discovery rate (FDR) correction. Log2 fold change shrinkage was applied using the apeglm algorithm. The miRNA with FDR ≤ 0.1 were identified as differentially expressed. The BAM files were deposited in Sequence Read Archive (SRA) (BioProject ID: PRJNA1285677) with accession numbers SRR34351822-SRR34351829.

Validation of miRNA-seq

The miRNA-seq results were validated by RT-qPCR on five representative miRNAs (hsa-miR-1246; hsa-miR-17-3p; hsa-miR-340-5p; hsa-miR-193a-5p; hsa-miR-146b-5p) using total RNA samples subjected to miRNA-seq (for hsa-miR-17-3p and hsa-miR-340-5p) or total RNA extracted from different biological replicates (for hsa-miR-1246, hsa-miR-193a-5p and hsa-miR-146b-5p). The miRNA expressions were assessed at 24–48 h post-infection, as indicated in Table 5. The cDNA was synthesized using TaqMan™ MicroRNA Reverse Transcription Kit (Thermo Fisher Scientific, MA, USA), using specific RT primer provided with the TaqMan MicroRNA Assay. Briefly, the RNA samples were freshly quantitated by Qubit 4 Fluorometer and the RNA HS Assay (Thermo Fisher Scientific, MA, USA), then 10 ng total RNA in a final volume of 15 µl were used for reverse transcription following manufacturer's protocol. The cDNA samples were stored at -20 °C until miRNA qPCR. Equal amounts of cDNA (1 µl cDNA template) were added to each reaction tube, containing TaqMan universal Master Mix II no UNG (Thermo Fisher Scientific, MA, USA) and specific TaqMan miRNA Assay (containing specific primers and probe) in a final volume of 15 µl. The reactions were carried out in triplicate using Quantstudio 5 instrument (Thermo Fisher Scientific, MA, USA). The mixtures were incubated at 95 °C for 10 min, followed by 40 cycles at 95 °C for 15 s, and 60 °C for 1 min. The fold changes were calculated by relative quantification using the 2^-ΔΔCt method. The data were normalized using hsa-miR-16-5p and the small nucleolar RNA RNU48 as reference genes. The relative gene expression was set to 1 for the non-infected samples (control).

Prediction of putative miRNA/mRNA interactions

Since current evidence suggests that target mRNA degradation contributes largely to the miRNA-induced silencing effects, we explored miRNA-mRNA interactions in U937 cells infected by *L. infantum* at 24 h and 48 h post-infection. To this end, we used mirDIP (microRNA Data Integration Portal; https://ophid.utoronto.ca/m

irDIP/) (Version 5.3.0.2), a web-based platform that allows for the identification of bidirectional overlapping interactions between miRNAs and mRNAs in *Homo sapiens*[57]. The mirDIP platform integrates multiple target prediction databases and provides a standardized score for each miRNA–transcript relationship. The previously published upregulated and downregulated mRNAs in *L. infantum*-infected U937 cells[23] were queried against downregulated and upregulated miRNAs, respectively, obtained from the same samples. In detail, at 24 h post-infection, 749 and 864 mRNAs previously found upregulated and downregulated in infected cells were queried against 10 and 24 downregulated and upregulated miRNAs. At 48 h post-infection, 124 and 330 mRNAs previously found upregulated and downregulated in infected cells were queried against 12 and 25 downregulated and upregulated miRNAs. The analysis was performed at high confidence level, taking into account target predictions in the top 5% and predicted by at least five different databases. This conservative approach was selected to reduce computational noise and prioritize targets with the strongest interaction evidence restricted to inverse expression relationships. To identify transcription factors among dysregulated genes, the list published by Lambert and colleagues was used[58]. A more focused analysis was performed using the lists of dysregulated genes enriched in specific pathways (i.e., cholesterol and lipid metabolism, VEGF-VEGFR2 and NF2EL2-related pathways) obtained by functional enrichment analysis performed in Metascape as described previously[23]. The miRNA-mRNA enrichment was assessed by comparing the proportion of predicted targets within the specific gene set against the proportion of targets within the background using Fisher's Exact Test. For each analysis, mRNAs were classified as either high-confidence miRNA targets or non-targets according to mirDIP predictions, and as belonging or not belonging to the gene set of interest. The proportion of predicted targets within each gene set was compared to the proportion observed in the reference background (e.g., 27667 genes included in mirDIP[57]. Odds ratios (OR) > 1 were interpreted as evidence of enrichment of predicted miRNA targets within the gene set.

The putative associations miRNA/mRNA were visualized utilizing the Cytoscape software package (version 3.10.2)[59], with each node colored based on the differential expression value (green: downregulated; red: upregulated). Node fill color reflects the $\log_2$ fold-change, with color gradients corresponding to the direction and magnitude of expression changes. The miRNAs were depicted as circular nodes and mRNAs as square nodes. Node size was scaled according to degree centrality, with larger nodes representing elements with a higher number of interactions, indicating regulatory importance within the network. This representation emphasizes miRNAs with multiple downstream targets and mRNAs regulated by more than one miRNA.

Statistical analysis

Data obtained by RT-qPCR were analyzed by Unpaired t test with Welch's correction. All data are presented as mean ± standard deviation (SD).

To evaluate the enrichment of miRNA target genes within the identified mRNA sets, two-tailed Fisher's exact tests were performed using a 2 × 2 contingency table. A p-value < 0.05 and an Odds Ratio (OR) > 1 were considered indicative of significant over-representation.

All statistical analyses were performed using Prism version 5.0 software (GraphPad, San Diego, CA, USA).

Data availability

All data generated or analyzed during this study are included in this published article (and its Supplementary Information files). The datasets generated and/or analysed during the current study are available in the Sequence Read Archive (SRA) (BioProject ID: PRJNA1285677; https://www.ncbi.nlm.nih.gov/bioproject/PRJNA1285677) with accession numbers SRR34351822-SRR34351829.

Received: 29 November 2025; Accepted: 16 March 2026
Published online: 27 March 2026

References

1. Verma, C. et al. Springer Nature Singapore,. Critical Roles of Micro-RNAs in the Pathogenesis and Immunoregulation of Leishmania Infection. in *Challenges and Solutions Against Visceral Leishmaniasis* 183–212 (2023). https://doi.org/10.1007/978-981-99-6999-9_9
2. da Silveira, W. A. et al. miRmapper: A Tool for Interpretation of miRNA–mRNA Interaction Networks. *Genes* **9**, 458 (2018).
3. Dexheimer, P. J., Cochella, L. & MicroRNAs From Mechanism to Organism. *Front. Cell. Dev. Biol.* **8**, 537579 (2020).
4. Lemaire, J. et al. MicroRNA Expression Profile in Human Macrophages in Response to Leishmania major Infection. *PLoS Negl. Trop. Dis.* **7**, e2478 (2013).
5. Atri, C. et al. Host–parasite interactions after in vitro infection of human macrophages by Leishmania major: Dual analysis of microRNA and mRNA profiles reveals regulation of key processes through time kinetics. *Microbes Infect* **27**, 105502 (2025).
6. Colineau, L., Lambertz, U., Fornes, O., Wasserman, W. W. & Reiner, N. E. c-Myc is a novel Leishmania virulence factor by proxy that targets the host miRNA system and is essential for survival in human macrophages. *J. Biol. Chem.* **293**, 12805–12819 (2018).
7. Diotallevi, A. et al. Leishmania Infection Induces MicroRNA hsa-miR-346 in Human Cell Line-Derived Macrophages. *Front. Microbiol.* **9**, 1019 (2018).
8. Silva, S. C. et al. Behavior of two Leishmania infantum strains-evaluation of susceptibility to antimonials and expression of microRNAs in experimentally infected J774 macrophages and in BALB/c mice. *Parasitol. Res.* **117**, 2881–2893 (2018).
9. Scaramele, N. F. et al. Leishmania infantum infection modulates messenger RNA, microRNA and long non-coding RNA expression in human neutrophils in vitro. *PLoS Negl. Trop. Dis.* **18**, e0012318 (2024).
10. Ovalle-Bracho, C., Franco-Muñoz, C., Londoño-Barbosa, D. & Restrepo-Montoya, D. Clavijo-Ramírez, C. Changes in Macrophage Gene Expression Associated with Leishmania (Viannia) braziliensis Infection. *PLoS One.* **10**, e0128934 (2015).
11. Muxel, S. M., Laranjeira-Silva, M. F., Zampieri, R. A. & Floeter-Winter, L. M. Leishmania (Leishmania) amazonensis induces macrophage miR-294 and miR-721 expression and modulates infection by targeting NOS2 and L-arginine metabolism. *Sci. Rep.* **7**, 44141 (2017).

12. Fernandes, J. C. R., Muxel, S. M., López-Gonzálvez, M. A., Barbas, C. & Floeter-Winter, L. M. Early Leishmania infectivity depends on miR-372/373/520d family-mediated reprogramming of polyamines metabolism in THP-1-derived macrophages. *Sci. Rep.* **14**, 996 (2024).
13. Jafarzadeh, A. et al. Bidirectional cytokine-microRNA control: A novel immunoregulatory framework in leishmaniasis. *PLOS Pathog.* **18**, e1010696 (2022).
14. Gharsallah, C. et al. Mapping changes of miRNA-mRNA networks in Leishmania-infected macrophages predicts regulatory miRNA-TF loops as novel targets of parasite immune subversion. *BIORXIV* 365–406. https://doi.org/10.1101/2024.03.24.586456 (2024).
15. Heberle, H., Meirelles, V. G., da Silva, F. R., Telles, G. P. & Minghim, R. InteractiVenn: a web-based tool for the analysis of sets through Venn diagrams. *BMC Bioinformatics.* **16**, 169 (2015).
16. Tamgue, O. et al. Non-Coding RNAs in the Etiology and Control of Major and Neglected Human Tropical Diseases. *Front Immunol* **12**, 703936 (2021).
17. Kim, G. et al. Hsa-miR-1246 and hsa-miR-1290 are associated with stemness and invasiveness of non-small cell lung cancer. *Lung Cancer*. **91**, 15–22 (2016).
18. Galluzzi, L. et al. Leishmania infantum Induces Mild Unfolded Protein Response in Infected Macrophages. *PLoS One*. **11**, e0168339 (2016).
19. Cai, Y. et al. MicroRNA-17-3p suppresses NF-κB-mediated endothelial inflammation by targeting NIK and IKKβ binding protein. *Acta Pharmacol. Sin*. **2021 4212 42**, 2046–2057 (2021).
20. Yang, X. et al. Both mature miR-17-5p and passenger strand miR-17-3p target TIMP3 and induce prostate tumor growth and invasion. *Nucleic Acids Res.* **41**, 9688–9704 (2013).
21. Cobos Jiménez, V. et al. Next-generation sequencing of microRNAs uncovers expression signatures in polarized macrophages. *Physiol. Genomics*. **46**, 91–103 (2014).
22. Kadl, A. et al. Identification of a Novel Macrophage Phenotype That Develops in Response to Atherogenic Phospholipids via Nrf2. *Circ. Res.* **107**, 737–746 (2010).
23. Diotallevi, A. et al. Transcriptional signatures in human macrophage-like cells infected by Leishmania infantum, Leishmania major and Leishmania tropica. *PLoS Negl. Trop. Dis.* **18**, e0012085 (2024).
24. Feketea, G. et al. A Review of Macrophage MicroRNAs' Role in Human Asthma. *Cells* **8**, 420 (2019).
25. Hirschberger, S., Hinske, L. C. & Kreth, S. MiRNAs: dynamic regulators of immune cell functions in inflammation and cancer. *Cancer Lett.* **431**, 11–21 (2018).
26. Chandan, K., Gupta, M. & Sarwat, M. Role of Host and Pathogen-Derived MicroRNAs in Immune Regulation During Infectious and Inflammatory Diseases. *Front. Immunol.* **10**, 502685 (2020).
27. Sheedy, F. J. & Turning Induction of miR-21 as a Key Switch in the Inflammatory Response. *Front. Immunol. 6*. **21**, 19 (2015).
28. Mayr, C. Evolution and Biological Roles of Alternative 3′UTRs. *Trends Cell. Biol.* **26**, 227–237 (2016).
29. Sourdin, L. et al. Strongly regulated transcription factors exert an outsized influence in microRNA-regulated networks. *Cell. Commun. Signal.* **24**, 63 (2025).
30. Liu, Z. P., Wu, C., Miao, H. & Wu, H. RegNetwork: an integrated database of transcriptional and post-transcriptional regulatory networks in human and mouse. *Database* bav095 (2015). (2015).
31. Luo, M. C. et al. Runt-related transcription factor 1 (RUNX1) binds to p50 in macrophages and enhances TLR4-triggered inflammation and septic shock. *J. Biol. Chem.* **291**, 22011–22020 (2016).
32. Cao, H. et al. Ligand-dependent corepressor (LCoR) represses the transcription factor C/EBPβ during early adipocyte differentiation. *J. Biol. Chem.* **292**, 18973–18987 (2017).
33. Pérez-Núñez, I. et al. LCOR mediates interferon-independent tumor immunogenicity and responsiveness to immune-checkpoint blockade in triple-negative breast cancer. *Nat. Cancer 2022*. **33** (3), 355–370 (2022).
34. Buxadé, M. et al. Gene expression induced by Toll-like receptors in macrophages requires the transcription factor NFAT5. *J. Exp. Med.* **209**, 379–393 (2012).
35. Baron, V. T., Pio, R., Jia, Z. & Mercola, D. Early Growth Response 3 regulates genes of inflammation and directly activates IL6 and IL8 expression in prostate cancer. *Br. J. Cancer* **112**, 755–764 (2015).
36. Kearney, S. J. et al. Type I IFNs Downregulate Myeloid Cell IFN-γ Receptor by Inducing Recruitment of an Early Growth Response 3/NGFI-A Binding Protein 1 Complex That Silences ifngr1 Transcription. *J. Immunol.* **191**, 3384–3392 (2013).
37. Yuan, L. et al. Antiinflammatory effects of the ETS factor ERG in endothelial cells are mediated through transcriptional repression of the interleukin-8 gene. *Circ. Res.* **104**, 1049–1057 (2009).
38. Rodríguez-Calvo, R., Tajes, M. & Vázquez-Carrera, M. The NR4A subfamily of nuclear receptors: potential new therapeutic targets for the treatment of inflammatory diseases. *Expert Opin. Ther. Targets*. **21**, 291–304 (2017).
39. Pan, H. et al. Ipr1 gene mediates innate immunity to tuberculosis. *Nature* **434**, 767–772 (2005).
40. Ettinger, N. A. & Wilson, M. E. Macrophage and T-Cell Gene Expression in a Model of Early Infection with the Protozoan Leishmania chagasi. *PLoS Negl. Trop. Dis.* **2**, 252 (2008).
41. Rodriguez, N. E., Chang, H. K. & Wilson, M. E. Novel Program of Macrophage Gene Expression Induced by Phagocytosis of Leishmania chagasi. *Infect. Immun.* **72**, 2111–2122 (2004).
42. Bove, G. et al. METTL16-mediated inhibition of MXD4 promotes leukemia through activation of the MYC-MAX axis. *Oncogene 2025 4443*. **44**, 4159–4172 (2025).
43. Martínez, C. R. & Ruiz, C. J. Alterations in Host Lipid Metabolism Produced During Visceral Leishmaniasis Infections. *Curr. Trop. Med. Rep.* **6**, 250–255 (2019).
44. Podinovskaia, M. & Descoteaux, A. Leishmania and the macrophage: a multifaceted interaction. *Future Microbiol.* **10**, 111–129 (2015).
45. Yao, Y., Yang, S., Bai, Y., Yuan, Z. & Yang, Z. m6A-methylated TAL1 exacerbates lipid accumulation in ethylene bisdithiocarbamate metabolite–induced anorectal malformations in rat fetuses via miR-205/LCOR signaling. *Ecotoxicol. Environ. Saf.* **302**, 118594 (2025).
46. Kim, S. et al. T-Cell Death-Associated Gene 51 Is a Novel Negative Regulator of PPARγ That Inhibits PPARγ-RXRα Heterodimer Formation in Adipogenesis. *Mol. Cells*. **44**, 1–12 (2021).
47. Yousof, T. R. et al. Restoration of the ER stress response protein TDAG51 in hepatocytes mitigates NAFLD in mice. *J. Biol. Chem.* **300**, 105655 (2024).
48. Villanueva-Cabello, T. M., Gutiérrez-Valenzuela, L. D., Salinas-Marín, R., López-Guerrero, D. V. & Martínez-Duncker, I. Polysialic Acid in the Immune System. *Front. Immunol.* **12**, 823637 (2022).
49. Chen, L. et al. Inhibition of Secretin/Secretin Receptor Axis Ameliorates NAFLD Phenotypes. *Hepatology* **74**, 1845–1863 (2021).
50. Yang, M. et al. The NF-κB-SLC7A11 axis regulates ferroptosis sensitivity in inflammatory macrophages. *Cell. Insight*. **4**, 100257 (2025).
51. Xu, L., Fang, H., Xu, D. & Wang, G. HIPK2 sustains inflammatory cytokine production by promoting endoplasmic reticulum stress in macrophages. *Exp. Ther. Med.* **20**, 171 (2020).
52. Lee, C. et al. Vascular endothelial growth factor signaling in health and disease: from molecular mechanisms to therapeutic perspectives. *Signal. Transduct. Target. Ther.* **10**, 170 (2025).
53. Kueanjinda, P., Roytrakul, S. & Palaga, T. A Novel Role of Numb as A Regulator of Pro-inflammatory Cytokine Production in Macrophages in Response to Toll-like Receptor 4. *Sci. Rep.* **51** (5), 12784 (2015).

54. Zhang, C., Li, X., Wen, P. & Li, Y. Ellagic acid improves osteoarthritis by inhibiting PGE2 production in M1 macrophages via targeting PTGS2. *Clin. Exp. Pharmacol. Physiol.* **51**, e13918 (2024).
55. Lima, J. F., Cerqueira, L., Figueiredo, C., Oliveira, C. & Azevedo, N. F. Anti-miRNA oligonucleotides: A comprehensive guide for design. *RNA Biol.* **15**, 338–352 (2018).
56. Castelli, G. et al. Cultivation of Protozoa Parasites In Vitro: Growth Potential in Conventional Culture Media versus RPMI-PY Medium. *Vet. Sci.* **10**, 252 (2023).
57. Tokar, T. et al. mirDIP 4.1—integrative database of human microRNA target predictions. *Nucleic Acids Res.* **46**, D360–D370 (2018).
58. Lambert, S. A. et al. *Hum. Transcription Factors Cell* **172**, 650–665 (2018).
59. Shannon, P. et al. Cytoscape: A Software Environment for Integrated Models of Biomolecular Interaction Networks. *Genome Res.* **13**, 2498–2504 (2003).

Acknowledgements
We thank Dr. Giuseppe Persico for expert advice and valuable input on the bioinformatic analysis pipeline.

Author contributions
AD, LG, FV, GC, FB contributed to design the work. AD, LG analysis/interpretation of data. LG drafting the work. AD, GB, SM, GC, FB contributed to acquisition, analysis/interpretation of data and revising the manuscript critically. LG, FV contributed to funding acquisition. All authors reviewed and edited the manuscript and approved the final version.

Funding
This work has been supported by the Italian Ministry of University and Research (MUR) under the PRIN 2022 programme, Project "The role of small RNA in human and canine Leishmania infantum infection: a one-health approach" Project id: 2022KH5MBK.

Declarations

Competing interests
The authors declare no competing interests.

Additional information
Supplementary Information The online version contains supplementary material available at https://doi.org/10.1038/s41598-026-45026-x.

Correspondence and requests for materials should be addressed to L.G.

Reprints and permissions information is available at www.nature.com/reprints.

Publisher's note Springer Nature remains neutral with regard to jurisdictional claims in published maps and institutional affiliations.